Vol. 3 No: 2 3rd year 2018 Al-Kut Univ. College Journal مجلة كلية الكوت الجامعة
ISSN: 2616 – 7808 (Online) and ISSN: 2414 – 7419 (Print) Pages 10 - 38

Semi-analytical Modeling of Intrachannel Nonlinearity Based on BPSK & OOK Techniques

Mahdi Zaman[a] , Ali Hadi Hassan Al-Batat[a] , Hassan Abid Yasser[a*]
[a] Department of Physics-College of Education-Mustansiriyah University, P.O.Box:46219, Baghdad, Iraq.
zaman_mahdi@yahoo.com
[a*]Department of Physics-College of Science-Thi-Qar University- Thi-Qar, Iraq.

Abstract

The properties of intra-channel four wave mixing (IFWM) nonlinearity in fiber-optics communication system using a semi-analytical model for distribution of chirped optical signals is investigated based on binary phase shift-keying (BPSK) and on-off keying (OOK) transmission techniques. In highly disperse single channel fiber, a signal pulse broadens clearly and the by, it interacts nonlinearly with a large number of neighboring signals. This behavior leads to create echo signals in "0" bit slots and amplitude jitter in "1" bits slots that can significant limit the system performance due to increasing bit error rate (BER). In our study optical distortion due additive white Gaussian noise (AWGN) is considered, where all the signals are suffering from the same probability of error caused by variance, and the numerical simulation is used to test validity of semi-analytical expression by Matlab programming.

الخلاصة:

تم دراسة خصائص اللاخطية لمزج اربعة موجات داخل القناة الناقلة (IFWM) لنظم اتصالات اللايف البصرية باستخدام نموذج شبه تحليلي لتوزيع الإشارات الضوئية التي تعاني من تولد (chirp) بالاستناد الى تقنيات النقل (BPSK) و (OOK). في الألياف شديدة التشتت ، تتوسع نبض الإشارة بشكل ملحوظ وبالتالي تتفاعل بشكل لاخطي مع عدد كبير من الإشارات المتجاورة. هذا السلوك يؤدي إلى تولد صدى إشارات في الفتحات "0" بت واضطراب في السعة للاشارت في الفتحات "1" بت والتي تحد وبشكل كبير من أداء النظام بسبب زيادة معدل أخطاء البتات (BER). في دراستنا هذه التشوه البصري بسبب الضوضاء الغاوسية البيضاء المضافة (AWGN) تم اعمادها، حيث تعاني كل الإشارات من نفس احتمالية الخطأ الناتج عن التباين حيث تم استخدام المحاكاة العددية لاختبار صلاحية التعبير شبه التحليلي باستخدام برمجة المتالاب.

Keywords: Intrachannel nonlinearity; Four-wave-mixing; Dispersion management; RZ modulation format.

1. Introduction

Transmission of Return-to-zero (RZ) pulses in strongly dispersion management (DM) fibers is a key technology in high bit rate optical communication systems. Strong DM is found to manage fiber nonlinearity and suppress certain nonlinear effects. Such systems are, hence, commonly referred to as quasi- or pseudo-linear systems [1]. In quasi-linear system, the fiber nonlinearity can be considered as a small perturbation in the linear system. Since the dispersive effects are dominant in quasi-linear system, adjacent pulses are overlapping; hence, such system is also known as a strongly pulse-overlapped system [2]. The overlapping with adjacent pulses of the same channel leads to create intrachannel nonlinearity effects. Intrachannel four wave mixing (IFWM) is major source of nonlinearity impairments in high bit RZ transmissions systems (≥ 40 Gb/s), which is a phase-sensitive process through which power is transferred from groups of pulses within a channel to specific bit slot locations which result in echo pulses and amplitude jitter [3, 4]. Such highly dispersed ultralong-haul systems are on-off key (OOK) and binary phase shift keying (BPSK) [5].

Generally, the quasi-linear systems use compensated dispersion technique at the beginning or at the end of the span or of the entire link. As the bit rate increases, it is necessary to transmit shorter pulses, which have a broader spectrum and are, therefore, rapidly spread by the transmission fiber dispersion [6]. In OOK and BPSK transmission systems, information is carried by the intensity of the signal. Thereby, the phase of the signal has an extra degree of freedom. One major advantage of BPSK system improves receiver sensitivity in the linear regime compared to OOK system. However, IFWM introduces pattern-dependent nonlinear phase shifts to the OOK and BPSK signals [7].

The nonlinear interaction due to the overlap between adjacent signal pulses in single channel fibers, leads to create echo pulse in “0” slot and amplitude jitter in “1” slot induced by IFWM [8]. In Ref. [8], analytical expressions of IFWM is derived using a first order perturbation theory. In [9], a general first order perturbation theory for signal propagation in fiber-optic links is developed. The suppression of IFWM has drawn significant interest using phase coding technique in [10].

In this paper, we investigated the effect of chirp on the amount of echo pulses generated by IFWM. we estimated the magnitude of this effect on the BER in OOK and BPSK transmission systems using statistical model. The simulation is executed by Matlab program.

This paper is organized as follows: a coherent state of data signal is explained and how its effect on various types of modulations in section 2. a perturbed nonlinear Schrodinger equation in DM systems is derived for a Gaussian pulse to get more accurate visual result calculation. In sections 3 and 4, IFWM impairments based on BPSK and OOK modulations have been discussed and analytical description for variances of bit "0" and bit "1" for dispersion-managed coherent fiber-optic systems based on BPSK modulation are derived too. The signal distortion measurement in section 5, is studied by evaluating signal-to-noise ratio (SNR), the bit error rate (BER) and performances of binary digital communication systems. In section 6 we discuss our results of effects many parameters such chirp, dispersion, pulse bandwidth, length of span, and symbol rate on IFWM nonlinearity.

2. Perturbed Nonlinear Schrodinger Equation

Considering a single-mode channel of a fiber optic system, the evolution of optical pulses along channel with initial width $T_0 > 5$ps is governed by the nonlinear Schrödinger equation (NLSE) as

$$\frac{\partial u}{\partial z} + i\frac{\beta''}{2}\frac{\partial^2 u}{\partial t^2} = i\gamma(z)|u|^2 u \tag{1}$$

where $\gamma(z) = \gamma_0 e^{-\int_0^z \alpha(z')dz'}$ is the nonlinear coefficient and $\alpha(z)$ is the fiber attenuation coefficient and u is the electric field envelope, β'' is the second order dispersion parameter [11]. For interacted pulses transmit through a multi span link with perfect compensated dispersion per span, the field can be decomposed as a sum of fields of individual pulses for an input signal. Consequently, the signal at the transmitter is given by

$$u(z,t) = \sqrt{P_0} \sum_{n=-\infty}^{\infty} a_n f(t - nT_b) \tag{2}$$

where P_0 is the launch power, nT_b is the symbol bit interval, are the random variables depending on modulation transmission technique, and $f(t - nT_b)$ is the pulse profile shape [12].

Conventional single-channel systems are characterized by a large amount of chromatic dispersion. The optical pulses with a time width of a few picoseconds of such systems undergo a strong broadening and consequent pulses overlapping [13]. Since the dispersion length is much shorter than the nonlinear length, the nonlinearity can be considered as a small perturbation compared with the pulse distortion caused by dispersion [14]. Hence, the analytical insights into the effect of nonlinearity using perturbation theory is

$$u(z,t) = \sum_{n=-\infty}^{\infty} a_n u_n + \Delta u \tag{3}$$

where u_n is the linear solution to the NLSE (obtained by setting $\gamma_0 = 0$) and Δu is the perturbation due to Kerr nonlinearity. In order to obtain accurate and more realistic calculations, we must take into account that the parameter is very important called “chirp’. The chirp is a signal in which the frequency increases or decreases with time. Chirped pulses can be effect on nonlinear compensation, because as soon as the chirped pulses are launched into a fiber with a high value of dispersion its energy is spread for multiple times slots and in terms of power the signal is average making its almost flat [15].

2.1. Mathematical Model of Perturbation in Time Domain

Let's suppose the input pulse signal profile has an initial source chirp, the interaction along haul of propagation distance z for serial bits' pulses leads to linear solution [16]

$$u(z,t) = \frac{T_0\sqrt{P_0}}{T_1}\sum_n a_n \exp\left[-\frac{1+iC}{2}\frac{(t-nT_b)^2}{T_1^2}\right] \quad (4)$$

where $T_1^2 = T_0^2 - iD(1+iC)$, T_0 is the half width at $1/e$ intensity, C is the initial input chirp, and $D(z) = \int_0^z \beta'' dz'$ is the dispersion over a period z. By substituting Eq. (3) in (1) through (4), the modified perturbation NLSE will has the form

$$\frac{\partial \Delta u}{\partial z} + i\frac{\beta''}{2}\frac{\partial^2 \Delta u}{\partial t^2} = i\gamma(z)\sum_{l,m,n=-s}^{s} a_l\, a_m\, a_n^* u_l u_m u_n^* = iF(z,t) \quad (5)$$

where l, m and n are the interacted pulses locations. Here, we assume intrachannel nonlinearity is only contribution by neighboring s bits on both sides of central bit, i.e., $(l,m,n) \in [-s,s]$. The right-hand side of Eq.(5) represents effects of intrachannel nonlinearity which may be identified as follows; The case $l = m = n$ corresponds to Intrachannel self-phase modulation (ISPM), the case $l = n \neq m$ or $l \neq n = m$ to intrachannel cross-phase modulation (IXPM), and the case $l \neq m \neq n$ to non-degenerate IFWM and $l = m \neq n$ to degenerate IFWM [17]. In order to obtain the perturbation part which represents the effects of nonlinearity or the variance between the input and output signals, the differential Eq. (5) is solved, to get

$$\Delta\tilde{u}(L_{tot},\omega) = i\int_0^{L_{tot}} \tilde{F}(\omega, z)\exp[-iD(z)\omega^2/2]\,dz \tag{6}$$

where L_{tot} is the total transmission distance. Here, if we have perfect dispersion per span with constant loss α and dispersion parameter β'', we would have the case $D(z) = \beta'' z$.

By taking the Fourier transform of nonlinear force of Eq. (6), $F(z,t)$, we obtain

$$\tilde{F}(z,\omega) = \frac{\gamma(z)P_0^{\frac{3}{2}}T_0^3}{|T_1|^2 T_1}\sqrt{\frac{\pi}{\mathcal{E}_1(z)}}\sum_{l,m,n=-s}^{s} a_l a_m a_n^*\, e^{-\mathcal{E}_3(z)+\frac{[\mathcal{E}_2(z)+i\omega]^2}{4\mathcal{E}_1(z)}}. \tag{7}$$

If we use the perturbation analysis description, the perturbation term $x_{l,m,n}$ should be obtained by the weighted summation of three-symbol-products[18]. The nonlinear perturbation coefficient of pulses located at lT_b, mT_b, and nT_b generate an echo pulse centered approximately at $(l+m-n)T_b = jT_b$, where $j \in [-s, s]$; More generally, the generated echo pulses have distribution probability for all possible signal locations. Due to symmetry, the ensemble average of the nonlinear distortion should be the same on each symbol interval [17]. Therefore, the dominant contributions to the nonlinear distortion at $t = 0$ come from the symbol slots that satisfy $(l+m-n=0)$ when time shift is constant.

Substituting Eq. (7) in (6), and after performing the inverse Fourier transformation for centered echo pulse at $t = 0$, leads to

$$\Delta u(L_{tot},t) = \gamma_0 P_0^{3/2} \sum_{l,m,n=-s}^{s} a_l a_m a_n^* x_{lmn}(L_{tot},t) \quad (8)$$

where x_{lmn} is the nonlinear perturbation coefficient that is given by

$$x_{lmn}(L,t) = i \int_0^{L_{tot}} \frac{e^{-\alpha z - \mathcal{E}_3 + \mathcal{E}_2}}{\sqrt{1 + 2i\mathcal{E}_1 D}}\, dz \quad (9)$$

where we have special case parameters as

$$\mathcal{E}_1 = \frac{3T_0^2 + iK}{2[(T_0^2 + DC)^2 + D^2]}, \quad (10a)$$

$$\mathcal{E}_2 = \frac{(\mathcal{E}_4)^2}{4\mathcal{E}_1}\left(1 - \frac{1}{1 + 2i\mathcal{E}_1 D}\right), \quad (10b)$$

$$\mathcal{E}_3 = \frac{T_0^2[(l^2 + m^2) + ml(1 - iK/T_0^2)]T_b^2}{[(T_0^2 + DC)^2 + D^2]}, \quad (10c)$$

$$\mathcal{E}_4 = \frac{2T_0^2(l + m)T_b}{[(T_0^2 + DC)^2 + D^2]}, \quad (10d)$$

and

$$K = D + C(T_0^2 + DC). \quad (10e)$$

These conditions correspond to the IFWM terms that lead to perturbation in amplitude (amplitude jitter) and energy transfer which add linear part is not effect on spectrum of enveloped pulses. However, the total field at the end of the transmission line is [19]

$$u(L_{tot}, t) = P_0^{1/2}\left[a_0 f(t) + \sum_{n=-s, n\neq 0}^{s} a_n f(t - nT_b)\right]$$
$$+\gamma_0 P_0^{\frac{3}{2}} \sum_{l,m,n=-s}^{s} a_l a_m a_n^* x_{lmn}(L_{tot}, t) \tag{11}$$

where $f(t)$ is the incident field profile of linearly chirped Gaussian pulses which is given by [20]

$$f(t) = \exp\left(-\frac{(1 + iC)t^2}{2T_0^2}\right) \tag{12}$$

The first term of Eq. (11) represents the average power of the transmitted bit. The second term on the right-hand side represents the intersymbol interference (ISI) from the neighboring symbols, and the last term on the right-hand side represents the nonlinear distortion due to ISPM, IXPM, and IFWM. SPM and IXPM are independent of bit pattern and only lead to deterministic changes to the first order. When the launch power is too large, the depletion of the pump pulses due to IFWM cannot be ignored and as a result, the peak powers of the pulses vary leading to IXPM penalty which is bit pattern dependent. However, the ISPM and IXPM of a constant intensity modulation such BPSK and OOK can be removed by the electrical equalizer. So, we ignore them in any nonlinear effects calculations.

3. Variance Calculation of BPSK Modulation System

When the noise of matched filter is neglected, the random variable of output signals for the binary modulation techniques is modeled as

$$a_n = a_{In} + i a_{Qn} \qquad n = 0,1, \dots, \mathcal{N} \tag{13}$$

where In and Qn are the transmitted symbol of in-phase and quadrature component, respectively, and $\mathcal{N}$ is the number of samples during the observation interval. In the case of BPSK constellation, the imaginary part of Eq. (3.19) is zero. So, $a_n = a_n^*$ and a_n's are the symbols taking the value of ± 1 with equal probability to be 1 or -1 [21]. Practically, After passing through the ideal unite gain coherent detector, the output signal is multiple by the $\sqrt{P_0}\, f^*(t)$ and integrated over one bit interval which is equivalent to the matched filter receiver. Then, the output function of the correlator can be represent by a function of transmitted random binary variables I which is symbolize photocurrent. $a_0 = 1$, it will be decided that bit "1" is transmitted. Otherwise, bit "0" is transmitted or $a_0 = -1$. However, with a stable phase of BPSK systems, the photocurrent at $t = 0$ is proportional to the output power signal of correlator as [19]

$$P \propto I^2(L_{tot}, 0) = |u_0(L_{tot}, 0)|^2 + 2\gamma \mathcal{R}e\{u_0(L_{tot}, 0) u_1^*(L_{tot}, 0)\} \\ + \gamma^2 |u_1(L_{tot}, 0)|^2. \qquad (14)$$

The terms on the right-hand side of Eq. (14) are the received currents due to a linear transmission, correlated signal–nonlinear distortion, and the nonlinear distortion. So, the intrachannel nonlinear effect may be represented by variance of current in the end of transmission line as

$$I = I_0 + \delta I \qquad (15)$$

where

$$I_0 = \pm P_0^{1/2} \pm \gamma_0 \left(x_{000} + 2 \sum_{m=-s, m\neq 0}^{s} x_{0mm} \right) \qquad (16)$$

and

$$\delta I = P_0^{1/2} \sum_{n=-s,n\neq 0}^{s} a_n x_{\mathrm{lin},n} + \gamma_0 P_0^{3/2} \sum_{\substack{l,m,n=-s,l\neq 0 \\ ,m\neq 0,l+m-n=0}}^{s} a_l a_m a_n^* x_{lmn}. \tag{17}$$

Both ISPM with index values ($l = m = n = 0$) and IXPM with index values ($l = 0,\ m = n$) are independent of bit pattern and only lead to deterministic changes to launched power represented by the first term. Therefore, they do not contribute to the variance. The first and second terms in Eq. (17) represent the linear and IFWM distortion, respectively. Linear part and IFWM make a major contribution to the calculations of variance and all the other triplets in Eq. (15) can be ignored in calculations.

The nonlinear distortion involving a_l, a_m, and a_n, leads to random fluctuations of the received signal. So for more accurate we have

$$\delta I = \delta I_{\mathrm{lin}} + \delta I_{\mathrm{IFWM,d}} + \delta I_{\mathrm{IFWM,nd}} \tag{18}$$

where $\delta I_{\mathrm{lin}}, \delta I_{\mathrm{IFWM,d}},$ and $\delta I_{\mathrm{IFWM,nd}}$ represent random current due to linear ISI, degenerate IFWM (D-IFWM), and non-degenerate IFWM (ND-IFWM), respectively [22]. The non-degenerate symmetric IFWM triplet involving the pump pulse in bit slot $l + m - n = 0$ is responsible for making the probability density function (PDF) asymmetric. An IFWM triplet is degenerate if $l = m$. However, the PDFs become nearly symmetric as amplified spontaneous emission (ASE) noise increases. Consequently, Eq. (17) can be represented as follows

$$\delta I_{\mathrm{lin}} = P_0^{1/2} \sum_{n=-s,n\neq 0}^{s} a_n x_{\mathrm{lin},n}\ , \tag{19}$$

$$\delta I_{\mathrm{IFWM,d}} = \gamma_0 P_0^{3/2} \sum_{\substack{l,n=-s \\ ,l+m-n=0,l=m}}^{s} a_n x_{lln} \ , \tag{20}$$

and

$$\delta I_{\mathrm{IFWM,nd}} = \gamma_0 P_0^{3/2} \sum_{\substack{l,m,n=-s \\ ,l+m-n=0,l<m}}^{s} a_l a_m a_n^* x_{lmn} . \tag{21}$$

In an optical receiver containing a Gaussian noise n_f, the variance of random serial bits ‘±1’ in a direct detection BPSK system

$$\sigma_{BPSK}^2 = \sigma_{\mathrm{IFWM,lin}}^2 + \sigma_{n_f}^2 \tag{22}$$

where $\sigma_{\mathrm{IFWM,lin}}^2$ and $\sigma_{n_f}^2$ are the variance of both IFWM and linear part of input function distribution, and ASE noise after the matched filter [23]. In quantum physics, concept of coherence state describes all properties of the correlation between physical quantities of a single wave, or between several waves or wave packets [24]. So, the variance of $\delta I_{\mathrm{IFWM,lin}}$ can be written as

$$\sigma_{\mathrm{IFWM,lin}}^2 = \langle [\delta I_{\mathrm{lin}} + \delta I_{\mathrm{IFWM,d}} + \delta I_{\mathrm{IFWM,nd}}]^2 \rangle$$
$$- \langle [\delta I_{\mathrm{lin}} + \delta I_{\mathrm{IFWM,d}} + \delta I_{\mathrm{IFWM,nd}}] \rangle^2 \tag{23}$$

where $\langle . \rangle$ denotes the ensemble average which involve about probability distribution density of transmitted signal. The overlapping states caused by perturbation in transmitted signal leads several cases of random variables. For BPSK, the random variables of overlapping states are

$$\langle a_n \rangle = 0, \tag{24}$$

$$\langle a_m a_n^* \rangle = \begin{cases} 1, & \text{if } m = n \\ 0, & \text{othewise} \end{cases}, \tag{25}$$

$$\langle a_l a_m a_{l+m}^* \rangle = \begin{cases} 1, & \text{if } l = 0 \text{ or } m = 0 \\ 0, & \text{othewise} \end{cases}, \tag{26}$$

and

$$\langle a_l a_m a_{l+m}^* a_{l'} a_{m'} a_{l'+m'}^* \rangle = \begin{cases} 1, \text{if } l = l' \text{ or } m = m' \\ 1, \text{if } l = m' \text{ or } m = l' \\ 0 \quad \text{othewise} \end{cases}. \tag{27}$$

Using Eqs. (24-26), it is easy to show that

$$\langle [\delta I_{\text{lin}} + \delta I_{\text{IFWM,d}} + \delta I_{\text{IFWM,nd}}] \rangle = 0. \tag{28}$$

3.1. ISI

Let us first consider the average square of linear part of signal perturbation, as

$$\begin{aligned} \langle \delta I_{\text{lin}}^2 \rangle &= \sum_{\substack{m,n=-s \\ m\neq 0, n\neq 0}}^{s} \langle a_m a_n^* \rangle x_{\text{lin},m} x_{\text{lin},n}^* \, \delta_{nm} \\ &= P_0 \sum_{m=-s, m\neq 0}^{s} e^{-\frac{m^2 T_b^2}{T_0^2}}. \end{aligned} \tag{29}$$

where the overlapping between neighboring signals would be to the same level.

3.2. D-IFWM

The perturbation will make mix in state levels, so we have to assume that every random variable of such states a_s may be in $a_{s'}$ degenerated state. Hence, the average square of variance of D-IFWM will be

$$\langle \delta I_{\text{IFWM,d}}^2 \rangle = \gamma_0^2 P_0^3 \sum_{\substack{l+m-n=0 \\ ,l=m}} \sum_{\substack{l'+m'-n'=0 \\ ,l'=m'}} \langle a_l^* a_{l'} a_l^* a_{l'} a_n^* a_{n'} \rangle \, x_{lln} \, x_{l'l'n'}^* \delta_{ll'} \delta_{nn'}$$

$$= \gamma_0^2 P_0^3 \sum_{2l=n} |x_{lln}|^2. \tag{30}$$

where $\langle a_n a_{n'}^* \rangle$ =1, and n has to be matched to n'. Otherwise, means we have orthogonal quantum state which leads to zero value of $\langle \delta I_{\text{IFWM,d}}^2 \rangle$. Thereby, to satisfy $l + m = n$ and $l' + m' = n'$ in case $l = m$ and $l' = m'$, we should put $m = m'$.

3.3. ND-IFWM

The average square of variance of ND- IFWM is

$$\langle \delta I_{\text{IFWM,nd}}^2 \rangle = \gamma_0^2 P_0^3 \sum_{\substack{l+m-n=0 \\ ,l<m}} \sum_{\substack{l'+m'-n'=0 \\ ,l'<m'}} \langle a_l a_{l'}^* a_m a_{m'}^* a_n^* a_{n'} \rangle$$

$$\times x_{lmn} x_{l'm'n'}^* (\delta_{ll'} \delta_{mm'} \delta_{nn'} + \delta_{ml'} \delta_{lm'} \delta_{nn'}). \tag{31}$$

Since summation carried out over the region of $l < m$, the factor 2 introduce in ND- IFWM. So, Eq. (30) is simplified as

$$\langle \delta I_{\text{IFWM,nd}}^2 \rangle = 2\gamma_0^2 P_0^3 \sum_{l+m-n=0, l<m} |x_{lmn}|^2. \tag{32}$$

3.4, ISI and D-IFWM Correlation

The correlation between linear part of signal perturbation and D-IFWM can be obtained by calculating the magnitude of overlap between the two cases quantity as

$$\langle \delta I_{\text{IFWM,d}} \delta I_{\text{lin}} \rangle = \gamma_0 P_0^2 \sum_{\substack{n=-s, l=m \\ ,l+m-n=0}}^{s} \sum_{n'=-s}^{s} \langle a_l^2 a_n a_{n'}^* \rangle \mathcal{R}e\{x_{lln} x_{\text{lin},n'}^*\} \delta_{nn'}$$

$$= \gamma_0 P_0^2 \sum_{n=-s}^{s} e^{-\frac{n^2 T_b^2}{T_0^2}}. \tag{33}$$

3.5. ISI and ND-IFWM Correlation

Taking the overlapping between linear part of perturbed state and ND-IFWM, to get

$$\langle \delta I_{\mathrm{IFWM,nd}} \delta I_{\mathrm{lin}} \rangle = \gamma_0 P_0^2 \sum_{\substack{n=-s, l<m \\ , l+m-n=0}}^{s} \sum_{n'=-s}^{s} \langle a_l a_n^* a_m a_{n'}^* \rangle$$
$$\times \mathcal{R}e\{x_{lmn} x_{\mathrm{lin},n'}^*\} \delta_{lm} \delta_{nn'} = 0. \tag{34}$$

3.6. D-IFWM and ND-IFWM Correlation

The magnitude of overlapping between D-IFWM and ND-IFWM is

$$\langle \delta I_{\mathrm{IFWM,d}} \delta I_{\mathrm{IFWM,nd}} \rangle = \gamma_0 P_0^2 \sum_{\substack{l+m-n=0 \\ , l=m}} \sum_{\substack{l'+m'-n'=0 \\ , l'<m'}} \langle a_l a_{l'}^* a_l a_{m'}^* a_n^* a_{n'} \rangle$$
$$\times \mathcal{R}e\{x_{lln} x_{l'm'n'}^*\} \delta_{ll'} \delta_{lm'} \delta_{nn'} = 0. \tag{35}$$

Finally, the total variance impairments based on BPSK modulation system is

$$\sigma_{IFWM,\mathrm{lin}}^2 = \langle \delta I_{\mathrm{lin}}^2 \rangle + \langle \delta I_{\mathrm{IFWM,d}}^2 \rangle + \langle \delta I_{\mathrm{IFWM,nd}}^2 \rangle$$
$$+2\langle \delta I_{IFWM,d} \delta I_{\mathrm{lin}} \rangle. \tag{36}$$

Simulation of Eq. (36) gives a good perception about intrachannel nonlinear distortion thereby SNR and BER calculations.

4. Variance Calculation of OOK Modulation System

Let us consider a direct detection OOK system. Eq. (15) can be rewritten as

$$I = I_0 + \delta I_{\mathrm{lin}} + \delta I_{\mathrm{nl}} \tag{37}$$

where

$$I_0 = P_0^{1/2} + \gamma_0 P_0^{3/2}\left(x_{000} + 2\sum_{m=-s,m\neq 0}^{s} x_{0mm}\right), \tag{38}$$

$$\delta I_{\text{lin}} = P_0^{1/2}\sum_{n=-s,n\neq 0}^{s} a_n x_{\text{lin},n}, \tag{39}$$

and

$$\delta I_{\text{nl}} = \gamma_0 P_0^{3/2}\sum_{\substack{l,m,n=-s\\ ,l+m-n=0}}^{s} a_l a_m a_n^* x_{lmn}. \tag{40}$$

The three terms of Eq. (38) do not contribute to the distribution of variance as we mentioned previously. The coherent state of data signals gives random variables of which effect on modulation system performance of optical detector.

For OOK, the random variables are

$$\langle a_n \rangle = 1/2\,, \tag{41}$$

$$\langle a_m a_n^* \rangle = \begin{cases} 1/4, & \text{if } n \neq m \\ 1/2, & \text{if } n = m \end{cases}. \tag{42}$$

So, in direct detection OOK system, the average square of variance of linear current distortion is

$$\langle \delta I_{\text{lin}}^2 \rangle = P_0 \sum_{\substack{m,n=-s\\ m\neq 0,n\neq 0}}^{s} \langle a_m a_n^* \rangle\, x_{\text{lin},m}\, x_{\text{lin},n}^*\, \delta_{nm}$$

$$= \frac{1}{2}P_0 \sum_{\substack{n=-s\\ n\neq 0}}^{s} \left|x_{\text{lin},n}\right|^2 + \frac{1}{4}P_0 \sum_{\substack{m,n=-s\\ m\neq 0,n\neq 0}}^{s} x_{\text{lin},m}\, x_{\text{lin},n}^*, \tag{43}$$

and

$$\langle \delta I_{\mathrm{lin}} \rangle^2 = \frac{1}{4} P_0 \sum_{\substack{n=-s \\ n\neq 0}}^{s} \left| x_{\mathrm{lin},n} \right|^2. \tag{44}$$

Thereby, the variance of ‘1’ bit for OOK transmission technique due to linear distortion is

$$\sigma_{\mathrm{lin}}^2 = \langle \delta I_{\mathrm{lin}}^2 \rangle - \langle \delta I_{\mathrm{lin}} \rangle^2$$

$$= \frac{1}{4} P_0 \sum_{\substack{n=-s \\ n\neq 0}}^{s} \left| x_{\mathrm{lin},n} \right|^2 + \frac{1}{4} P_0 \sum_{\substack{m,n=-s \\ m,n\neq 0, m\neq n}}^{s} x_{\mathrm{lin},m}\, x_{\mathrm{lin},n}^{*}. \tag{45}$$

Calculation of nonlinear distorsion depend on increasing of number degrees of degenerate and non-degenerate levels $r = (l, m, n)$ and $r' = (l', m', n')$ respectivly, then the square of average variance of nonlinear current distortion will be

$$\langle \delta I_{\mathrm{nl}} \rangle^2$$

$$= \gamma_0^2 P_0^3 \sum_{\substack{l+m-n=0 \\ ,l'+m'-n'=0}} \langle a_l a_m a_{l+m}^{*} \rangle \langle a_{l'}^{*} a_{m'}^{*} a_{l'+m'} \rangle\, x_{lmn}\, x_{l'm'n'}^{*} \delta_{ll'} \delta_{mm'} \delta_{nn'}$$

$$= \gamma_0^2 P_0^3 \sum_{l+m-n=0} \frac{1}{2^{2r}} \left| x_{\mathrm{lin},n} \right|^2. \tag{46}$$

The average of square variance of nonlinear current distortion is

$$\langle \delta I_{\mathrm{nl}}^2 \rangle = \gamma_0^2 P_0^3 \sum_{\substack{l+m-n=0 \\ ,l'+m'-n'=0}} \frac{1}{2^{x}}\, x_{lmn}\, x_{l'm'n'}^{*} (\delta_{ll'} \delta_{mm'} \delta_{nn'} + \delta_{ll'} \delta_{mm'} \delta_{nn'})$$

$$= \gamma_0^2 P_0^3 \sum_{\substack{l+m-n=0 \\ ,l'+m'-n'=0}} \frac{1}{2^{x-1}}\, x_{lmn}\, x_{l'm'n'}^{*}. \tag{47}$$

Where we used the following random varibles of OOK modulation data signals

$$\langle a_l a_m a_{l+m}^* \rangle = \begin{cases} 1/2^r = 1/4, & \text{if } l = m \\ 1/2^r = 1/8, & \text{if } l \neq m \end{cases}, \tag{48}$$

$$\langle a_l a_m a_{l+m}^* a_{l'}^* a_{m'}^* a_{l'+m'} \rangle = \left\{ \frac{1}{2^x} \right. . \tag{49}$$

where x is a function of (l, m, n, l', m', n') index.

In the Eq. (48) r represent the number non-degenarated degrees of the set index (l, m) where $(l + m = n)$. In the Eq. (3.53) x represent the number non-degenarated degrees of the set index (l, m, l', m') where $(l + m = n)$ and $(l' + m' = n')$. Thereby, the variance nonlinear distortion may estimate by following equation

$$\sigma_{\text{nl}}^2 = \langle \delta I_{\text{nl}}^2 \rangle - \langle \delta I_{\text{nl}} \rangle^2. \tag{50}$$

Finally, the total variance in OOK modulation techinique is

$$\sigma_{\text{OOK}}^2 = \sigma_{\text{lin}}^2 + \sigma_{\text{nl}}^2 + \sigma_{n_f}^2. \tag{51}$$

Due to considering only AWGN channel, the last term in right hand of Eq. (51) that represent the ASE noise filter which is neglected in simulation calculations of intrachannel nonlinear distortion. These results provide good approximations to calculate SNR and BER.

5. The signal distortion measurement

In addition to nonlinear and dispersion effects there are some parameters, such as, modulations techniques and filtering can affect the transmission quality and accuracy of the received message [25]. Modulation is some kind of digital signal processing in terms of optimizing the performance of digital communication systems [26]. Because of imperfections in a digital communication system during data leads to errors. The logic level 1 can be received as a logic level 0 and vice versa. Usually, the number of errors that are likely to occur in the system is expressed as the BER, that should be lower than a given limit. BER define mathematically, as the number of bit errors divided by the total number of transferred bits during a studied time interval [27].

A commonly used criterion is that among 10^9 bits at most one bit may on average be incorrectly transmitted, which corresponds to a BER < 10^{-9}. To evaluate the BER performance of binary digital communication systems, the statistics of the signal distortion can be assumed to be Gaussian, a signal quality measure known as error function. When the decision threshold is optimized the BER corresponding to a given Q-value is [28]

$$BER = \frac{1}{2} erfc\left(\frac{Q}{\sqrt{2}}\right) \approx \frac{exp\left(-\frac{Q^2}{2}\right)}{\sqrt{2\pi}Q}. \tag{52}$$

5.1. SNR Calculations

The probability error (Pe) is the expectation value of the BER, so the BER can be considered as an approximate estimate of the Pe. This estimate is accurate for a long time interval and a high number of bit errors. The signal to noise ratio (often abbreviated SNR) is measure used in science and engineering to quantify how much a signal has been corrupted by noise [27]. It is defined as ratio of data set or average power relative to average noise power that represented by the total variance [29]

$$SNR = \frac{P_0}{1.88\, \sigma_{tot}^2}. \tag{53}$$

5.2. BER Calculations

The Probability distribution of a signal pulse noise is assumed to be Gaussian. For a set threshold level, the BER of $\mathrm{RZ-OOK}$ modulation system as a function of SNR can be expressed as [30]

$$BER_{(RZ-OOK)} = \frac{1}{2}\operatorname{erfc}\left(\frac{Q_{(RZ-OOK)}}{\sqrt{2}}\right) \tag{54}$$

where

$$Q_{(RZ-OOK)} = \sqrt{\frac{SNR}{2}}\ . \tag{55}$$

The BPSK modulation system is the simplest form of phase shift keying; it is the most robust of all the PSKs since it takes the highest level of noise or distortion to make the demodulator reach an incorrect decision. The BPSK equation of BPSK modulation can be expressed as a function of SNR as [31]

$$BER_{(BPSK)} = \frac{1}{2}\operatorname{erfc}\left(\frac{Q_{(BPSK)}}{\sqrt{2}}\right) \tag{56}$$

where

$$Q_{(BPSK)} = \sqrt{SNR}\,. \tag{57}$$

6. Results and Discussions

For BPSK technique, calculation of IFWM variance is obtained by using the numerical simulation of Eq. (34), while for OOK technique we used Eq. (51). On the other hand, the SNR and BER are obtained by using Eqs. (53-57). In all our calculations we ignore effects of ASE noise, and receiver noise to get more accurate results for IFWM variance, and thereby for calculations of SNR and BER. The specific parameters used in our numerical simulation are listed in Table (1).

The tests proved that parameters give a better possible quality of system performance. These parameters may vary depending on the study of the characteristics of each parameter. The essential condition for evaluating the performance of any communication system is that the amount of SNR must be high Decreasing effects of intrachannel nonlinearity in single core fiber and performance improvement is achieved by choosing better simulation parameters. Figures (1-2) show the effects of number of interacted signals and initial chirp C on SNR; for OOK and BPSK modulation techniques, using different values of pulse width T_0.

Table 1. Simulation Parameters for Gaussian Pulses.

Parameter	Value	Unit
β''	-7	$\mathrm{ps}^2/\mathrm{km}$
L	80	km
γ	1.1	$\mathrm{W}^{-1}/\mathrm{km}$
α	0.0461	1/km
T_b	25	ps
T_0	8	ps
P_0	0.3	mW
β_c''	18	$\mathrm{ps}^2/\mathrm{km}$
C	-0.3	non

Fig. 1 shows SNR versus number of interacted adjacent signals. As can be seen, SNR decreases dramatically as variance. This is because of the interaction closed neighbor signals is increasing and hence, the nonlinear interaction is growing. For OOK modulation, due the distribution accounts for echo pulses are more complex compared to BPSK, SNR for location periods $(l, m, l+m \leq |15|)$ is not accurate. For BPSK, the decreasing of SNR reach to certain of value about location periods ($l, m, l+m \leq |10|$). However, for both systems OOK and BPSK, results show the stability of the nonlinear interaction of adjacent signals location at ($l, m, l+m \geq |15|$). However, it clearly appears that the interaction of neighboring pulses has a limited range leading to decrease the BER to a certain value, and then it tends to stability. This behavior is physically acceptable due to decreasing effect of far located pulses on central pulse.

Fig. 2 shows the SNR as a function of chirp pulse, where inline nonlinearity compensation for transmission distance of 80 Km is achieved. We found for OOK technique, when the chirp is ranging between -0.2 and -0.3, the SNR has the maximum values. For BPSK, chirp has obvious effect where maximum values of SNR at chirp range between zero and +0.2. Otherwise, chirp effect causes negatively of performance of transmission system. Generally, in all cases of our simulations, we have find out the best performance among other initial pulse-width is about $T_0 = 8ps$ and SNR of OOK is better than BPSK about 6 dB. However, in the OOK technique, the SNR tends to a higher value at a negative chirp values and vs for BPSK where SNR tends to higher value at positive chirp values.

The quality of the communications system is restricted by a bit error rate (BER$\leq 10^{-9}$). Since the intrachannel nonlinearity is the main factor in the systems of high bit transmissions systems that leads to increasing in BER, so we studied the relationship between the BER and the related parameters of OOK and BPSK techniques. Figures (3-6) explain the effects of launch power P_0, initial pulse-width T_0, compensated dispersion $\beta_c^{"}$, and dispersion $\beta^{"}$ parameters on Bit Error Rate (BER), respectively.

Fig. 3 explains the dependence of the BER on P_0 for single-span fiber system with compensated dispersion; and T_0 with 6, 7, 8, 9ps were considered. We found that the minimum discrepancy between the OOK and BPSK appears at maximum value of P_0. As the peak power increases, the BER is grew logarithmically leading to bond the performance of transmission system. The optimum selected parameters are achieving BER less than 10^{-10}.

Fig. 4 shows the minimum BER versus T_0 for several values of practical interested launch power P_0. As can be seen, For OOK technique the curve is shifted at minimum BER from initial pulse-width $T_0 = (8 - 8.8)ps$ where launch power is ranging $P_0 = (0.3 - 0.6)mW$, respectively. But the curve is shifted at minimum BER, for BPSK technique, from initial pulse-width $T_0 = 8.5ps$ to $T_0 = 9ps$ where launch power is ranging $P_0 = (0.3 - 0.6)mW$, respectively.

Fig.5 illustrates the BER of transmitted signals in single-mode fiber, after compensating for $\beta_c^{''}$. For the OOK system, the BER decreases slowly with increasing of the $\beta_c^{''}$ parameter. When the dispersion is about $\beta_c^{''} = 18ps^2/km$, provided dispersion leads to slightly reduction of nonlinear effects. Beyond $\beta_c^{''} = 18ps^2/km$, BER grows rapidly which leads to increase of the IFWM efficiency. Same behavior from BPSK system is appear but the lower BER is about $\beta_c^{''} = 14ps^2/km$. However, the OOK system shows higher BER than BPSK system in all various cases of initial pulse-width T_0.

Fig. 6 shows the BER as a function of $\beta^{''}$. For OOK and BPSK systems, when the dispersion is small, BER is at lower value due to redaction of the variance of the nonlinear distortion. This is because the pulses do not broaden significantly, so there is no significant overlap between neighboring pulses and there is less nonlinear interaction. Balancing between effects of T_0 and $\beta^{''}$

leads to less BER around $T_0 = 8ps$ and $\beta'' = -7ps^2/km$, where the discrepancy between BER of BPSK and the OOK is less than 25%.

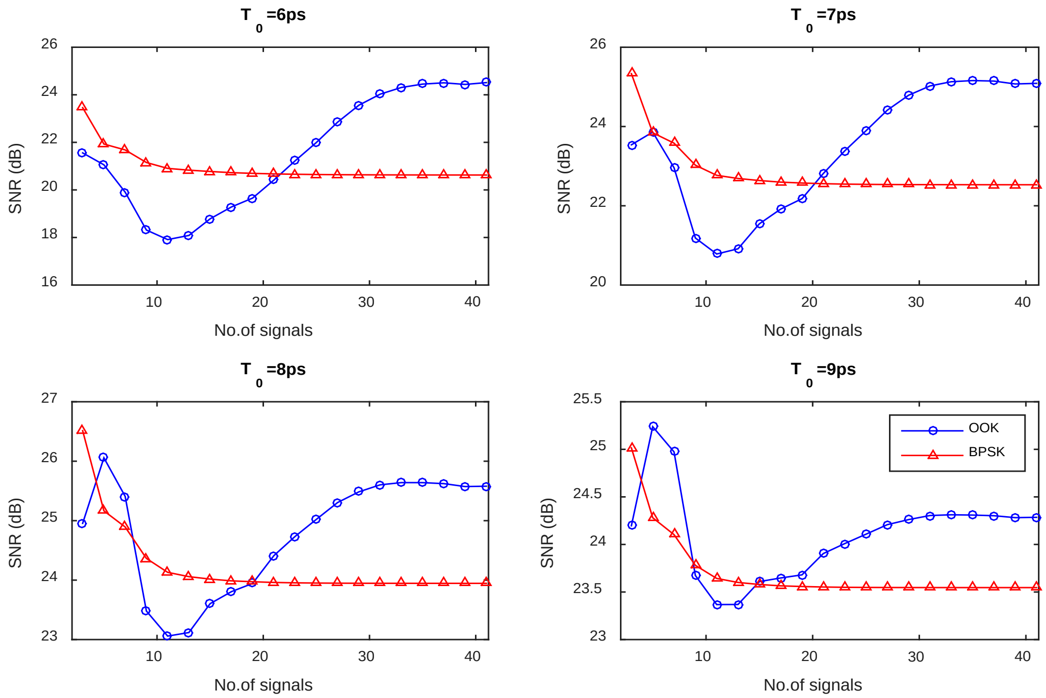

Fig. 1. SNR vs. number of interacted neighboring signals for OOK and BPSK modulation systems.

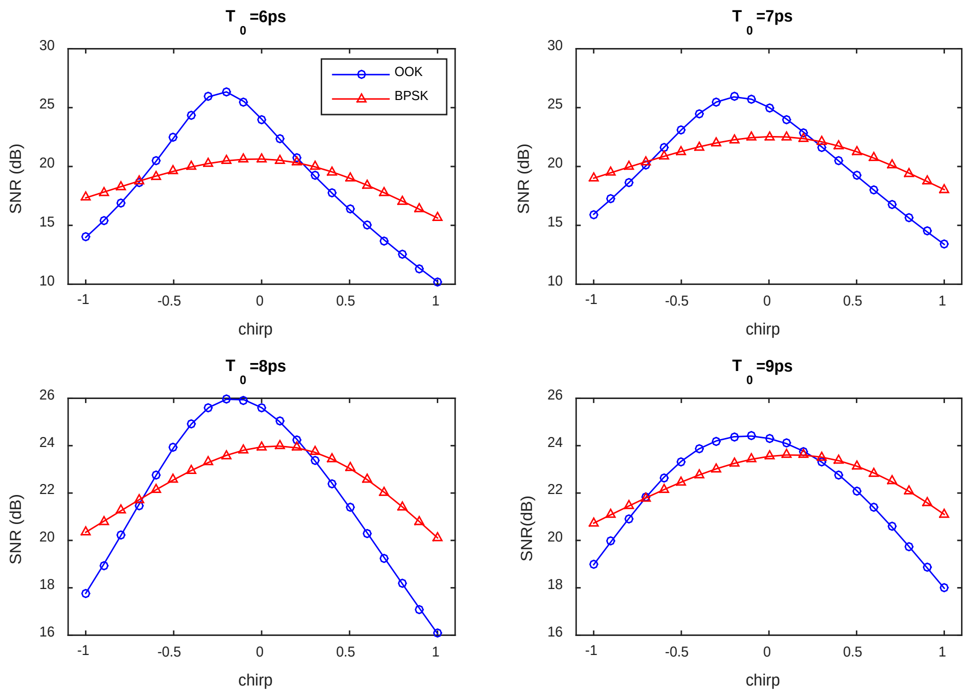

Fig. 2. SNR as a function of chirp pulse for OOK and BPSK modulation systems.

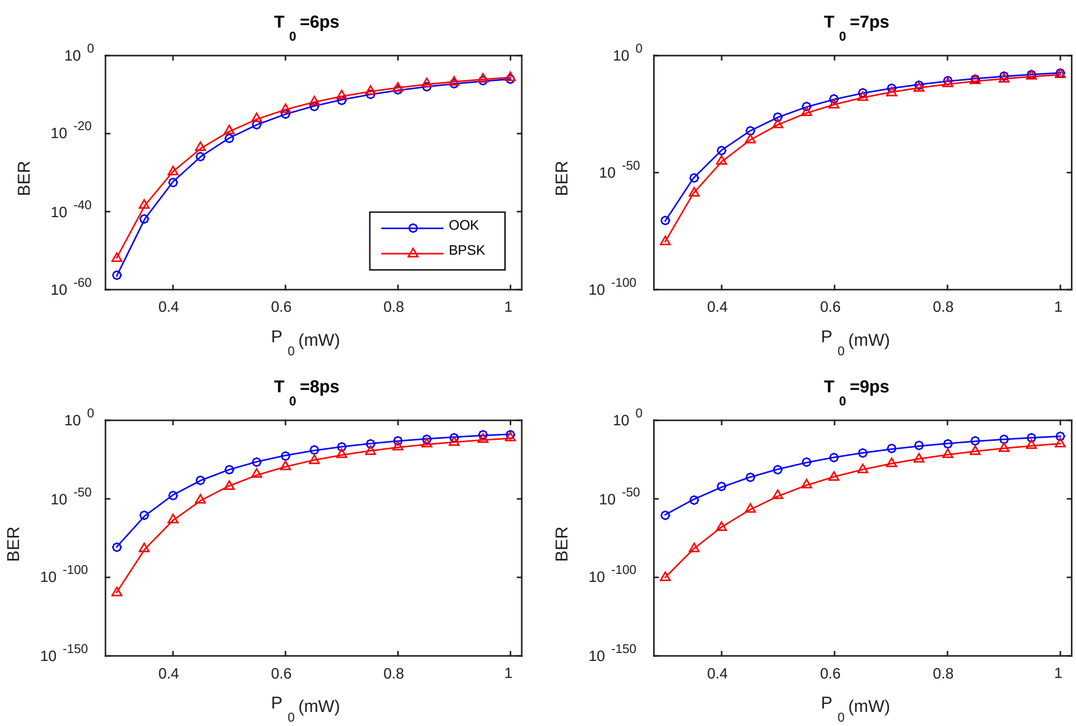

Fig. 3. BER vs. launch power for OOK and BPSK modulation techniques.

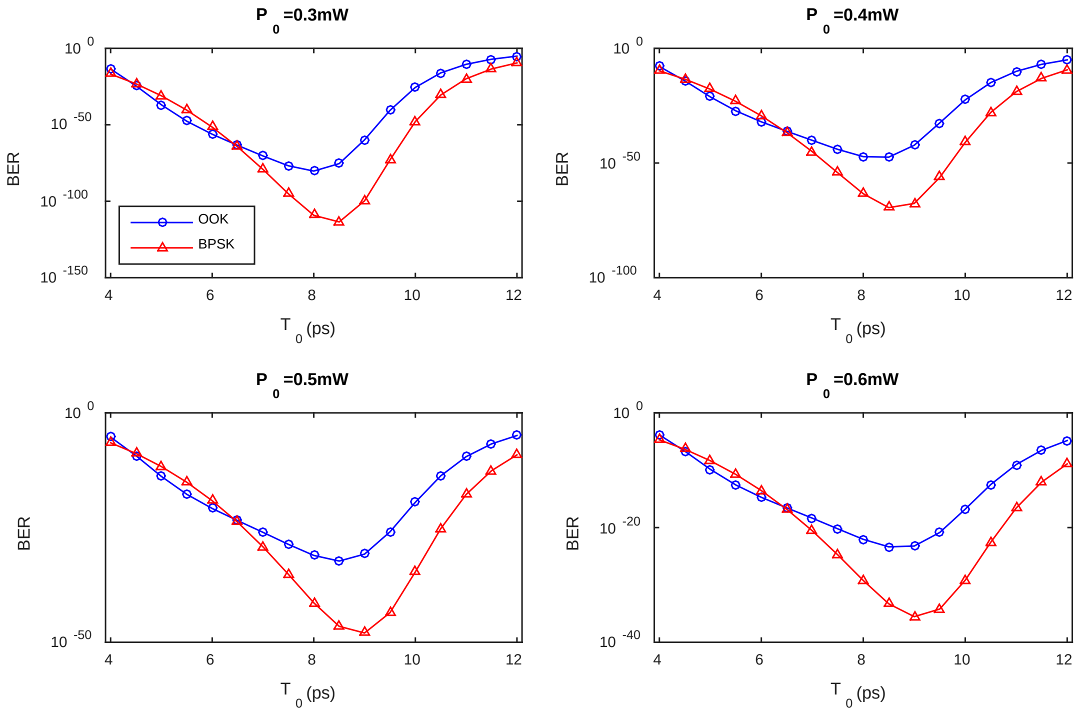

Fig. 4. BER as a function of initial pulse-width for OOK and BPSK modulation techniques.

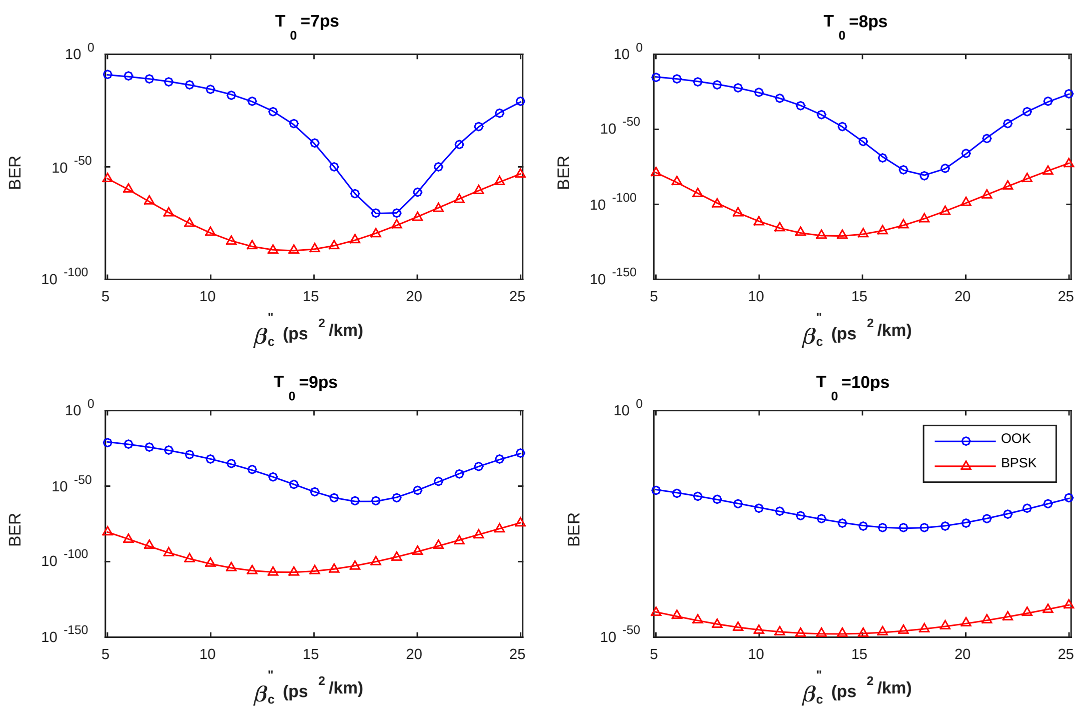

Fig. 5. BER vs. compensated dispersion parameter for OOK and BPSK transmission techniques.

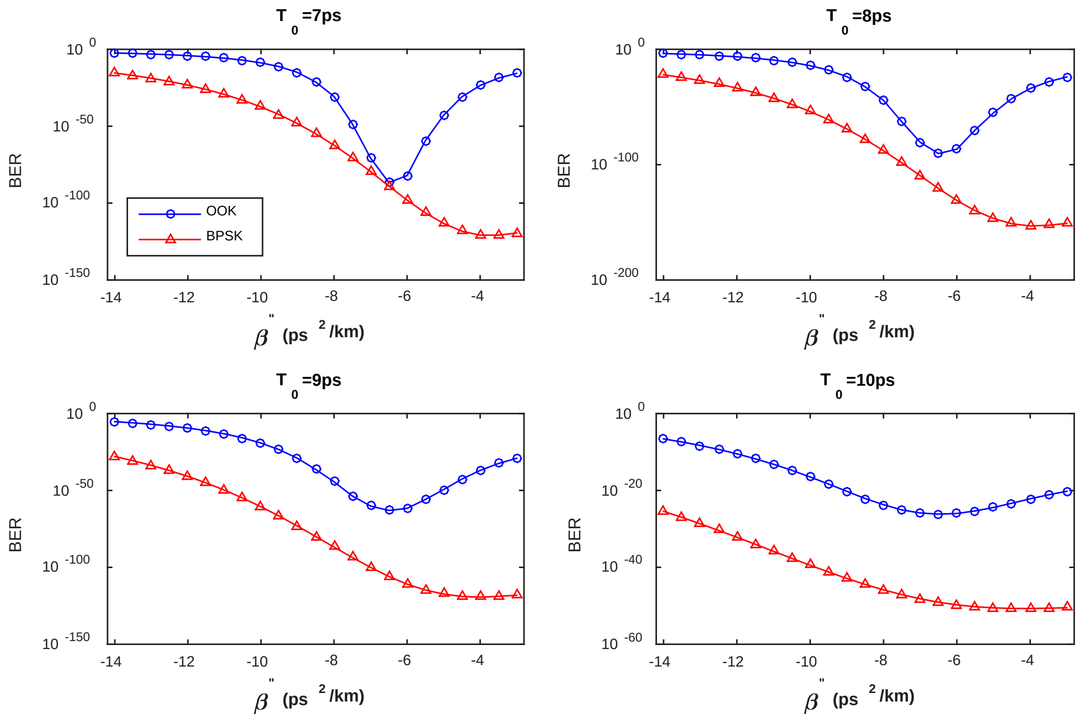

Fig. 6. BER as a function of dispersion parameter for OOK and BPSK transmission techniques.

7. Conclusion

In this paper, we proposed a semi-analytical statistic model of the intrachannel nonlinearity effects in single fiber-optic channel based on OOK and BPSK transmission techniques. Numerical simulation showed by using appropriate parameters, it is possible to reduce the IFWM distortion, increase the ratio of transmitted information and decrease the error rate to acceptable values. The best performance of initial pulse width is obtained at ($T_0 \sim 8\,ps$), less or more than this value leads to increase neighboring signals overlap; thereby increase the overall variance. Also shown for all the cases the chirp is “zero” gives less BER as possible as, which is desired in transmission systems.

Acknowledgment

The author would like to thank Mustansiriyah University (www,uomustansiriyah,edu.iq) for their support in this research.

References

[1] M.J. Ablowitz, T. Hirooka, Resonant intrachannel pulse interactions in dispersion-managed transmission systems, IEEE J. Sel. Top. Quantum Electron. 8 (3) (2002) 603-615.

[2] M. Malekiha, Analysis of Nonlinear Effects and Their Mitigation in Fiber-Optic Communication Systems, PhD diss., 2011.

[3] S. Kumar, J.C. Mauro, S. Raghavan, D.Q. Chowdhury, Intrachannel nonlinear penalties in dispersion-managed transmission systems, IEEE J. Sel. Top. Quantum Electron. 8 (3) (2002) 626-631.

[4] H.G. Batshon, I.B. Djordjevic, B.V. Vasic, An Improved Technique for Suppression of Intrachannel Four-Wave Mixing in 40-Gb/s Optical Transmission Systems, IEEE Photonics Technol. Lett. 19 (2) (2007) 67-69.

[5] E. Ip, A. Lau, D. Barros, J. Kahn, Coherent detection in optical fiber systems, Opt. Express, 16 (2008) 753-791.

[6] A. Del Duce, R. I. Killey, P. Bayvel, Comparison of nonlinear pulse interactions in 160-Gb/s quasi-linear and dispersion managed soliton systems, IEEE J. Lightwave Technol. 22 (5) (2004) 1263-1271.

[7] K. Ho, Phase-Modulated Optical Communication Systems, first ed., Springer Science Media & Business Media, 2005.

[8] D. Yang, S. Kumar, Intra-Channel Four-Wave Mixing Impairments in Dispersion-Managed Coherent Fiber-Optic Systems Based on Binary Phase-Shift Keying, IEEE J. Lightwave Technol. 27 (14) (2009) 2916-2923.

[9] A. Mecozzi, R. J. Essiambre, Nonlinear shannon limit in pseudolinear coherent systems, IEEE J. Lightwave Technol. 30 (12) (2012) 2011-2024.

[10] Z. Tao, Y. Zhao, Y. Fan, L. Dou, T. Hoshida, J.C. Rasmussen, Analytical Intrachannel Nonlinear Models to Predict the Nonlinear Noise Waveform, IEEE J. Lightwave Technol. 33 (10) (2015) 2111-2119.

[11] L. Ladányi, Numerical studies of the nonlinear and dispersive propagation of optical pulses using the method of lines, Proc. SPIE vol., 8697 (2012).

[12] A.P.T. Lau, S. Rabbani, J.M. Kahn, On the Statistics of Intrachannel Four-Wave Mixing in Phase-Modulated Optical Communication Systems, IEEE J. Lightwave Technol. 26 (14) (2008) 2128-2135.

[13] S. Boscolo, C. Finot, Nonlinear Pulse Shaping in Fibres for Pulse Generation and Optical Processing, Int. J. Opt. 2012 (2012).

[14] A. Pizzinat, A. Schiffini, F. Alberti, et al., 40-Gb/s systems on G.652 fibers: comparison between periodic and all-at-the-end dispersion compensation, IEEE J. Lightwave Technol. 20 (9) (2002) 1673-1679.

[15] J. Prilepsky, S. Derevyanko, S. Turitsyn, Conversion of a chirped Gaussian pulse to a soliton or a bound multisoliton state in quasi-lossless and lossy optical fiber spans, J. Opt. Soc. Am., 24 (6) (2007) 1254-1261.

[16] G. Agrawal, Nonlinear Fiber Optics, four ed., Academic Press, 2013.

[17] S. Kumar, S. Shahi, D. Yang, Analytical modeling of a single channel nonlinear fiber optic system based on QPSK, Opt. Express 20 (25) (2012) 27740- 27755.

[18] Z. Tao, Y. Zhao, Y. Fan, L. Dou, T. Hoshida, J.C. Rasmussen, Analytical Intrachannel Nonlinear Models to Predict the Nonlinear Noise Waveform, IEEE J. Lightwave Technol. 33 (10) (2015) 2111-2119.

[19] S. Kumar, M. Jamal-Deen, Fiber Optic Communications Fundamentals and Applications, first ed., John Wiley & Sons, Ltd, 2014.

[20] G. Agrawal, Fiber–Optic Communication Systems, four ed., John Wiley & Sons, 2012.

[21] T. Moazzeni, Y Jiang, H Selvaraj, T. Chen, Analytical models for distribution of the envelope and phase of linearly modulated signals in AWGN channel, Int. J. Electron. Telecom. 60 (1) (2014) 70-73.

[22] S. Kumar, Analysis of degenerate four-wave-mixing noise in return-to-zero optical transmission systems including walk-off, IEEE J. Lightwave Technol. 23 (1) (2005) 310-320.

[23] J. Chitode, Communication Systems-1, third ed., Technical Publications Pune, 2008.

[24] M. Born, E. Wolf, Principles of Optics, seventh ed., Cambridge University Press, 1999.

[25] T. Hirooka, T. Nakada, A. Hasegawa, Feasibility of densely dispersion managed soliton transmission at 160 Gb/s, IEEE Photonics Technol. Lett. 12 (6) (2000) 633-635.

[26] K. Kikuchi, Fundamentals of Coherent Optical Fiber Communications, IEEE J. Lightwave Technol. 34 (1) (2016) 157-179.

[27] J. Alam, M. Alam, H. Guoqing, M. Mehrab, Improvement of Bit Error Rate in Fiber Optic Communications, Int. J. Future Comput. Commun. 3 (4) (2014) 281.

[28] P. Ramantanis, Contribution to the analysis of optical transmission systems using QPSK modulation, PhD diss., 2012.

[29] S. Naderi, Analysis and mitigation of the nonlinear impairments in fiber-optic communication systems, PhD diss., 2013.

[30] A. Majumdar, Advanced Free Space Optics (FSO): A Systems Approach, Springer Series in Optical Sciences, 2015.

[31] T. Y. Elganimi, Studying the BER performance, power- and bandwidth-efficiency for FSO communication systems under various modulation schemes, 2013 IEEE Jordan Conference on Applied Electrical Engineering and Computing Technologies (AEECT), Amman, 2013, pp. 1-6.